Deformation Capacity and Shear Strength of Fiber-Reinforced Cement Composite Flexural Members Subjected to Displacement Reversals

Gustavo J. Parra-Montesinos[1] and Praveen Chompreda[2]

Abstract: The behavior of fiber-reinforced cement composite (FRCC) flexural members under large displacement reversals was experimentally evaluated. Emphasis was placed on estimating the displacement capacity and shear strength of members constructed with strain-hardening FRCC materials. Two types of fibers were used: Ultrahigh molecular weight polyethylene fibers and steel hooked fibers in volume fractions ranging between 1.0 and 2.0%. The primary experimental variables were: (1) fiber type and volume fraction; (2) type of cement-based matrix (concrete or mortar); (3) average shear stress demand at flexural yielding; and (4) shear resistance provided through hoops versus total shear demand. All specimens constructed with a strain-hardening FRCC, with or without web reinforcement, exhibited drift capacities of at least 4.0%. A shear stress level of $0.30\sqrt{f'_c}$ [MPa] represented a lower bound for which no shear failure occurred in the strain-hardening FRCC test specimens, regardless of the member inelastic rotation demand. In addition, buckling of longitudinal reinforcement in the strain-hardening FRCC members without web reinforcement was not observed up to plastic hinge rotations of 4.0%.

DOI: 10.1061/(ASCE)0733-9445(2007)133:3(421)

CE Database subject headings: Fiber reinforced materials; Steel fibers; Earthquake resistant structures; Shear strength; Seismic design; Deformation; Displacement.

Introduction

Shear resisting mechanisms in reinforced concrete (RC) flexural members have been shown to degrade under inelastic displacement reversals (Wight and Sozen 1975; Scribner and Wight 1980; Aschheim and Moehle 1992; Priestley et al. 1994; Pujol 2002). This phenomenon is primarily caused by the opening of flexural-shear cracks as the member undergoes inelastic displacement reversals, which reduces aggregate interlock and shear carried in the member compression zone. In order to prevent shear failures in beam plastic hinge regions of earthquake-resistant structures, the American Concrete Institute (ACI) Building Code (2002) requires the use of sufficient transverse reinforcement to resist the total expected shear demand. This reinforcement is also intended to provide confinement to the concrete core and delay buckling of longitudinal bars. Thus, the ACI design approach for flexural members assumes no "concrete" contribution to shear strength, V_c, independent of the magnitude of earthquake-induced inelastic deformations.

During the past fifteen years, several models have been proposed for estimating the concrete contribution to shear strength of RC members, particularly columns, as a function of ductility demand (Aschheim and Moehle 1992; Priestley et al. 1994; Lehman et al. 1996; Martín-Pérez and Pantazopoulou 1998). Fig. 1 illustrates the ratio between concrete shear strength, V_c, and member shear strength when behaving elastically, $(V_c)_{\text{elastic}}$, versus displacement ductility obtained from the models proposed by Priestley et al. (1994) and Lehman et al. (1996). As can be seen, these models predict a reduction in the concrete shear resistance for increasing inelastic displacement demands, with a small residual strength at large ductility levels.

The need for substantial transverse steel reinforcement to provide shear resistance and confinement in regions of members expected to undergo inelastic deformations during an earthquake generally leads to reinforcement congestion, an increase in labor costs and difficulties during concrete casting. As an alternative to the use of closely spaced transverse reinforcement for the above purposes, the use of fiber-reinforced cement composites (FRCCs) was investigated in this research. It was expected that the increase in concrete ductility, both in tension and compression, due to the addition of fibers would allow a relaxation in transverse reinforcement detailing in RC flexural members while ensuring a stable behavior under large displacement reversals. In addition, with the increasing attention paid to the functionality of buildings shortly after earthquakes, the use of materials with high damage tolerance represents a viable option for achieving structures that would require little or no repairs after being subjected to a design-level earthquake (i.e., 10% probability of exceedance in 50 years).

Classification of Fiber-Reinforced Cement Composites

Because countless fiber-reinforced cement composites (FRCCs) can be obtained from the addition of fibers of different properties

[1]Associate Professor, Dept. of Civil and Environmental Eng., Univ. of Michigan, Ann Arbor, MI 48109-2125.

[2]Lecturer, Dept. of Civil Engineering, Mahidol University, Thailand.

Note. Associate Editor: Sashi K. Kunnath. Discussion open until August 1, 2007. Separate discussions must be submitted for individual papers. To extend the closing date by one month, a written request must be filed with the ASCE Managing Editor. The manuscript for this paper was submitted for review and possible publication on February 22, 2005; approved on November 14, 2005. This paper is part of the ***Journal of Structural Engineering***, Vol. 133, No. 3, March 1, 2007. ©ASCE, ISSN 0733-9445/2007/3-421–431/$25.00.

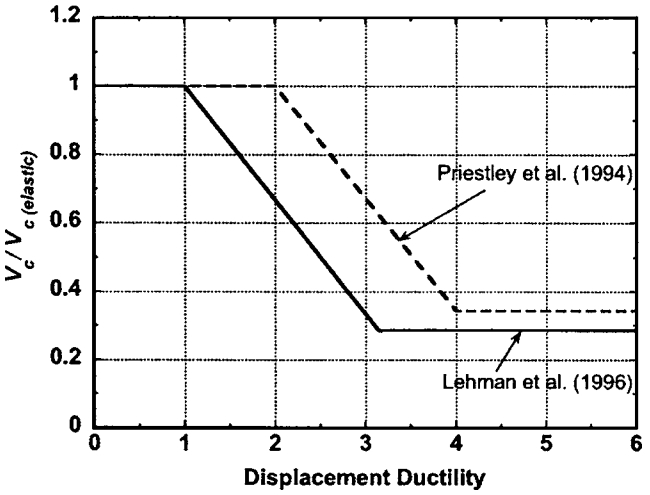

Fig. 1. Concrete shear strength decay with ductility

(material and geometry) and in various amounts to cement-based matrices, Naaman and Reinhardt (1996) proposed a classification system for FRCC materials based on their behavior under bending and direct tension. FRCCs are classified based on their bending behavior as either deflection-softening or deflection-hardening materials. A simply supported beam constructed with a deflection-softening material and tested up to failure would show a decay in load carrying capacity right after first cracking. On the other hand, a flexural member constructed with a deflection-hardening composite would sustain increasing amounts of loads after first cracking, as shown in Fig. 2. Deflection-hardening FRCCs, however, may exhibit substantially different responses under direct tension, leading to the definition of strain-softening and strain-hardening FRCCs. Similarly to deflection-softening FRCCs, a sample constructed with a strain-softening FRCC subjected to direct tension would exhibit a decay in tensile strength right after first cracking. In this case, damage localizes at the first crack and the stress versus strain response is dominated by crack opening. On the other hand, a strain-hardening FRCC specimen would exhibit a peak post-cracking strength greater than the first cracking strength, with multiple cracking pattern and a more uniform straining of the material.

Deflection-softening FRCCs are primarily used for cracking control and are not suitable for use in structural applications. On the other hand, the suitability of deflection-hardening FRCCs for use in structural applications depends on the expected load and deformation demands. In earthquake-resistant construction, where large tensile strain capacities are desirable, it is clear that strain-hardening FRCCs offer the best potential for enhancing structural behavior. However, for structural members subjected to gravity loads, the use of deflection-hardening and strain-softening materials is often sufficient for enhancing member shear strength and ductility.

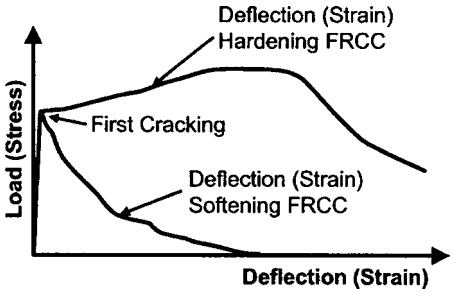

Fig. 2. Hardening and softening FRCCs based on their behavior under bending and direct tension

Fiber-Reinforced Cement Composites as Shear Reinforcement

For over thirty years the use of fiber-reinforced concretes or cement composites (FRCCs) as a means to enhance shear resistance in RC flexural members subjected to monotonic loads has been extensively investigated (for example, Batson et al. 1972; Mansur et al. 1986; Narayanan and Darwish 1987; Li et al. 1992; Schantz 1993; Adebar et al. 1997; Kwak et al. 2002). Most FRCCs used in those investigations contained deformed steel fibers (hooked or crimped) in volume fractions, V_f, between 0.5 and 1.5%. A common conclusion was that the addition of fibers to the concrete enhances shear strength and ductility of RC flexural members under monotonic loading and, in some cases, it leads to a change in failure mode from a brittle shear failure to a ductile flexural failure.

With regard to flexural members subjected to inelastic displacement reversals, most studies have focused on the use of regular fiber-reinforced concrete in beam plastic hinge regions as part of beam-column subassembly tests (for example, Henager 1977; Craig et al. 1984; Gefken and Ramey 1989; Filiatrault et al. 1995; Bayasi and Gebman 2002). In general, the cement composites used in these investigations consisted of regular concrete with steel fibers in volume fractions equal to or smaller than 2.0% and are believed to fall under the category of strain-softening FRCCs. Experimental results indicated that the addition of a relatively low volume fraction of fibers to the concrete may allow a relaxation of transverse reinforcement requirements (amount and spacing) in flexural members subjected to inelastic displacement reversals.

The seismic behavior of flexural members constructed with a strain-hardening FRCC known as Engineered Cementitious Composite or ECC (Li 1993) was investigated by Mishra and Li (1995) and Fischer and Li (2002). Results from these investigations showed that the use of ECC material enhances member ductility, shear strength and damage tolerance. Further, excellent behavior was observed in members without transverse steel reinforcement under relatively low shear stress levels (approximately $0.25\sqrt{f'_c}$ [MPa], where f'_c is the composite compressive strength). However, the use of FRCC materials to enhance shear resistance and displacement capacity in flexural members subjected to shear reversals of moderate to high intensity $0.25\sqrt{f'_c}$ to $0.50\sqrt{f'_c}$ [MPa], particularly those with a strain-hardening response, has not been evaluated in depth. Because of their superior post-cracking response compared to plain concrete, these materials represent a viable option to relax transverse reinforcement requirements in RC flexural members subjected to inelastic displacement reversals.

Tests of FRCC Members under Displacement Reversals

The behavior of FRCC members under displacement reversals was evaluated through the tests of eight specimens constructed with various fiber cementitious materials in the Univ. of Mich. Structures Laboratory. Each test specimen consisted of two can-

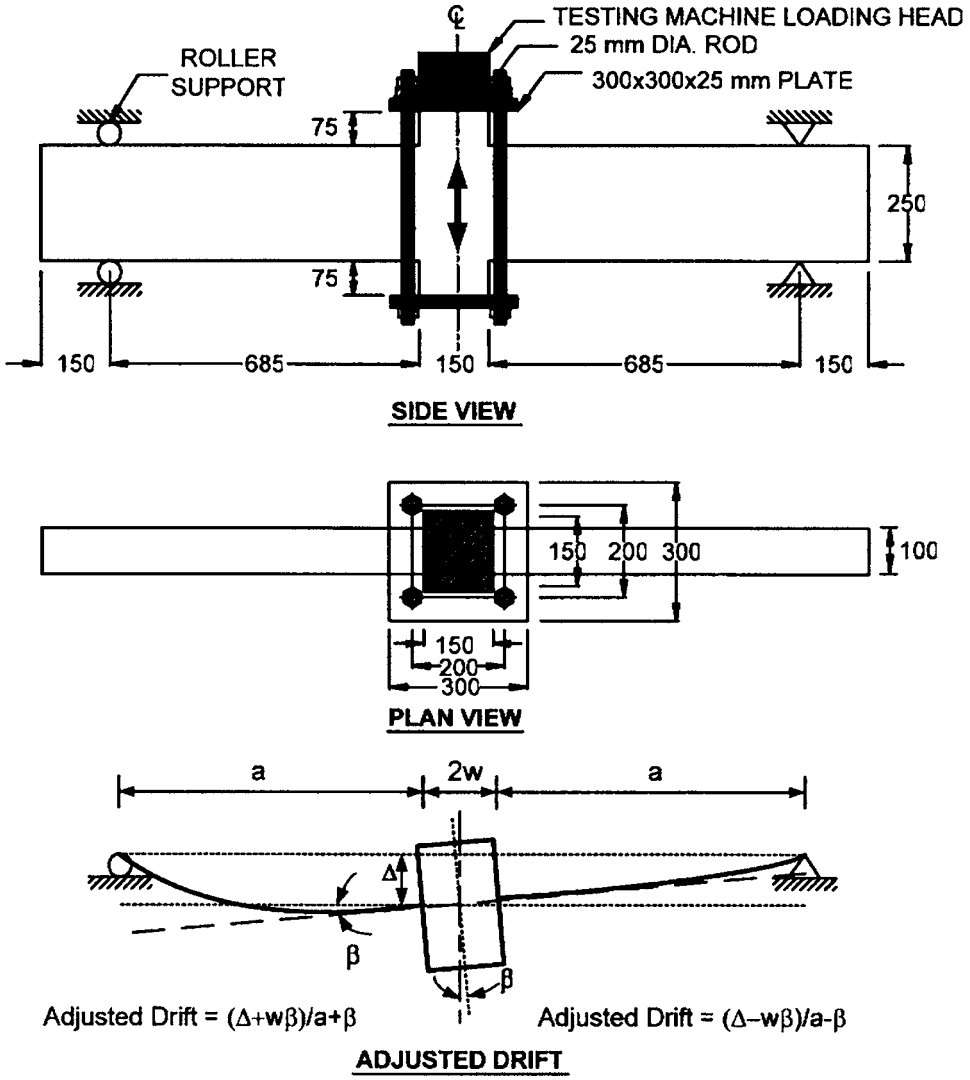

Fig. 3. Test configuration and calculation of member drift

tilever flexural members with a shear span-to-effective depth ratio of 3.0 connected through a stiff and strong middle block used for loading purposes. Fig. 3 shows the general specimen configuration and dimensions. The specimens were pin-supported at their ends (through restrained or free rollers directly in contact with the specimen), and vertical displacements were applied at the middle block through a hydraulic actuator. Each beam element had a cross section of 100×250 mm. Longitudinal reinforcement was placed in two layers (top and bottom) and the beam effective depth was 230 mm. It is worth mentioning that because of the use of closely spaced transverse reinforcement in critical regions of RC earthquake-resistant flexural members, multiple cracking develops at large displacements and thus, member size was not believed to significantly affect overall member behavior. Similarly, the enhanced cracking distribution that is typical of FRCC members, particularly those constructed with strain-hardening composites, would decrease any size effect in FRCC members. Therefore, the specimen dimensions were believed to be adequate for evaluating the behavior of FRCC flexural members under displacement reversals.

The main experimental variables investigated were: (1) fiber type and volume fraction, V_f, (2) type of cement-based matrix, (3) shear stress demand, and (4) v_s/v_u ratio, where v_s is the shear stress resisted by the transverse steel reinforcement at yielding assuming a 45 degree crack, and v_u is the average shear stress demand corresponding to the probable member moment strength, per Chapter 21 of the 2002 ACI Code (ACI 2002). Average shear stresses referred to in this investigation were calculated as V/bd, where V is the shear force, and b and d are the member width and effective depth, respectively. Table 1 summarizes the main features of each test specimen.

The first specimen was constructed with regular concrete and designed according to the provisions given in Chapter 21 of the 2002 ACI Building Code for earthquake-resistant construction. This specimen was used for comparison purposes with the FRCC specimens and its behavior should be representative of that expected in an RC flexural member designed according to modern codes when subjected to moderate shear stress reversals. The control RC specimen was reinforced with two #13M longitudinal bars in each layer (top and bottom), representing a tension steel reinforcement ratio, ρ, of 1.1%. The amount of longitudinal steel was selected such that a shear stress demand in the order of $0.30\sqrt{f'_c}$ [MPa] would be imposed on the member. Transverse reinforcement was designed to satisfy the total shear demand (i.e., $V_c=0$) and each layer consisted of two sets of steel wire (diameter

Table 1. Description of Test Specimens

	Cement matrix		Fiber		Longitudinal reinforcement				Transverse reinforcement				
Specimen	Type	f'_c [MPa]	Type	V_f (%)	Top and Bottom	ρ (%)	f_y [MPa]	f_u [MPa]	ϕ (mm)	s	f_y [MPa]	f_u [MPa]	v_s/v_u
RC-1.0-1.1	Concrete	38.4	—	—	2#13M	1.1	440	730	4	$d/4$	200	300	1.0
PE2.0-0-0.6	Mortar 1	55.7	PE[a]	2.0	2#10M	0.6	440	670	—	—	—	—	0
PE2.0-0-1.1	Mortar 1	44.4	PE	2.0	2#13M	1.1	440	730	—	—	—	—	0
PE1.5-0-1.1	Mortar 1	46.4	PE	1.5	2#13M	1.1	440	730	—	—	—	—	0
PE1.5-0.8-1.7	Mortar 1	50.3	PE	1.5	2#16M	1.7	445	710	6	$d/2$	590	800	0.8
SH2.0-0-1.1	Mortar 2	42.4	SH[b]	2.0	2#13M	1.1	440	730	—	—	—	—	0
SH1.5-0-1.1	Mortar 2	47.9	SH	1.5	2#13M	1.1	440	730	—	—	—	—	0
SH1.0-0.4-0.6	Concrete	34.7	SH	1.0	2#10M	0.6	440	670	4	$d/2$	200	330	0.4

[a]PE: Ultrahigh molecular weight polyethylene fibers.

[b]SH: Steel hooked fibers.

ϕ=4 mm) hoops spaced at $\frac{1}{4}$ of the member effective depth ($s=d/4$).

The test specimens constructed with FRCC materials were divided into two groups depending on the fiber type used. Four specimens were constructed with an FRCC reinforced with ultrahigh molecular weight polyethylene (Spectra) fibers in volume fractions of either 1.5 or 2.0%. The FRCC material in the remaining three specimens contained steel hooked (Dramix) fibers in volume fractions of either 1.0, 1.5 or 2.0%. Only one specimen in each of these two groups contained transverse steel reinforcement, spaced at half the member effective depth, as indicated in Table 1. The FRCC specimens were designed in flexure such that the shear stress demand at flexural capacity would range between approximately 0.15 and $0.40\sqrt{f'_c}$ [MPa], leading to longitudinal tension steel reinforcement ratios, ρ, of 0.6, 1.1, and 1.7%. To facilitate their identification, each specimen was labeled based on the material type (RC, PE, or SH for reinforced concrete, polyethylene FRCC and FRCC with steel hooked fibers, respectively), fiber volume fraction, v_s/v_u ratio, and longitudinal tension steel reinforcement ratio. Thus, Specimen SH2.0-0-1.1 refers to a specimen with 2.0% volume fraction of steel hooked fibers with $v_s/v_u=0$ (no transverse reinforcement), and a longitudinal reinforcement ratio equal to 1.1%. Because the RC control specimen did not contain fibers, it was labeled as RC-1.0-1.1.

Material Properties

The FRCC materials used in this investigation contained either ultrahigh molecular weight polyethylene (Spectra) fibers or steel hooked (Dramix) fibers. The polyethylene (PE) used in Spectra fibers has an elastic modulus of 117 GPa and a tensile strength of 2580 MPa. These fibers were straight with a diameter of 0.038 mm and a length of 13 mm, except for Specimen PE1.5-0.8-1.7, which contained 38 mm long fibers. The Dramix fibers, made of steel with minimum tensile strength of 1100 MPa, were 30 mm long and 0.55 mm in diameter with their ends hooked to improve bond with the matrix.

Two types of cement-based materials were used in the test specimens: Regular concrete and mortar. The regular concrete used in Specimens RC-1.0-1.1 and SH1.0-0.4-0.6 was supplied by a local ready-mix concrete company and contained coarse aggregate (limestone) with a 10 mm maximum size. The cement-based material used in the other six specimens was mortar, mixed in the Univ. of Mich. Structures Laboratory. The mixture proportions by weight for the mortar used in the FRCC materials with PE fibers (Mortar 1) were 1:0.4:1:0.15 for cement (Type III), water, Flint sand ASTM 30-70, and fly ash, respectively, while those used in the mortar with steel hooked fibers (Mortar 2) were 1:0.48:2:0.48. A high-range water reducing admixture was also added to ensure good workability of the composite. Fig. 4(a) shows typical compressive stress-strain responses obtained for the FRCC materials used in this investigation. The average compressive strengths measured within 24 h of the test are listed in Table 1. As shown in Fig. 4(a), the mortar FRCC materials exhibited a lower modulus of elasticity due to the lack of coarse aggregate in the mixture. However, these materials exhibited a post-peak response that resembled that of a well-confined concrete with strain capacities exceeding 1.0%.

In addition to compression tests, direct tensile tests of

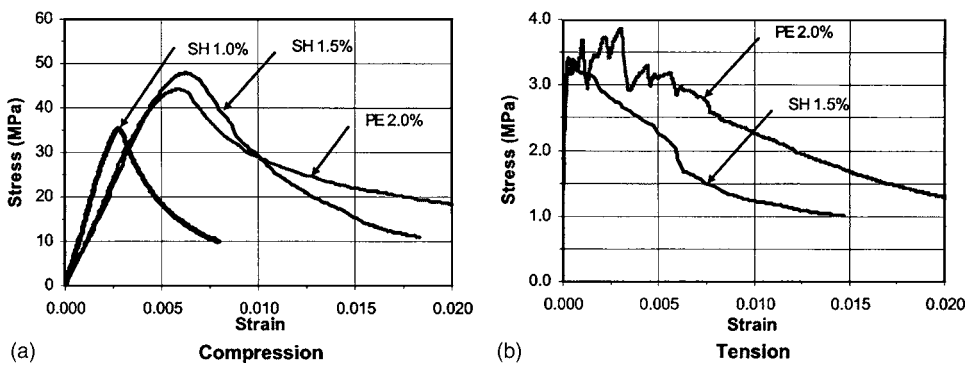

Fig. 4. Typical stress versus strain response of FRCCs

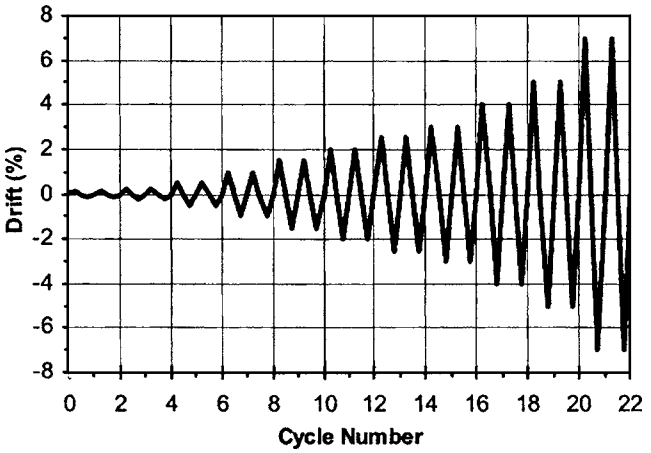

Fig. 5. Displacement demand history

13×50 mm and 25×50 mm "dog-bone" shaped specimens were conducted to classify the materials used as either strain-hardening or strain-softening composites. A strain-hardening tensile response was observed in the FRCCs with either 1.5 or 2.0% volume fraction of PE fibers and 2.0% volume fraction of steel hooked fibers. The strain at peak stress ranged between 0.3 and 0.5% with post-cracking strengths between 2.3 and 4.3 MPa. On the other hand, a strain-softening behavior was obtained when steel hooked fibers were used in volume fractions of 1.5% or less. Fig. 4(b) shows stress versus strain responses obtained from direct tension tests for the composites with 2.0% volume fraction of PE fibers (strain-hardening) and 1.5% volume fraction of steel hooked fibers (strain-softening).

Deformed Grade 420M steel reinforcing bars were used as longitudinal reinforcement for all eight specimens. The transverse reinforcement used in the RC control specimen and in Specimen SH1.0-0.4-0.6 was made out of 4 mm diameter steel wire, while 6 mm diameter smooth bars were used for the transverse reinforcement in Specimen PE1.5-0.8-1.7. The yield and ultimate strengths, f_y and f_u, respectively, obtained for the various types of steel used in this investigation are listed in Table 1.

Displacement Demand History and Instrumentation

The test specimens were subjected to a predetermined vertical displacement pattern applied at the middle block between the two cantilever members. Fig. 5 shows the displacement history planned for each test specimen as a function of average drift, which was calculated as the applied vertical displacement divided by the shear span of each cantilever member (685 mm). Because some rotation of the middle block occurred during the tests, the drift values measured in each cantilever segment were adjusted, as shown in Fig. 3. The applied vertical displacement and load were monitored through linear potentiometers and a load cell, respectively. Rotations in the middle block were measured through clinometers, while plastic hinge rotations and shear distortions were measured through linear potentiometers. The plastic hinge length was assumed to be equal to the member effective depth, d (230 mm), as suggested by Blume, Newmark, and Corning (1961). Strain gauges were used to monitor strains in the longitudinal and transverse reinforcement at the plastic hinge regions of the test specimens.

Performance of RC and FRCC Specimens under Displacement Reversals

Because each test specimen consisted of two cantilever members that may have been subjected to different drift demands due to rotations in the middle loading block, the drifts that will be referred to hereafter, unless indicated otherwise, correspond to those measured in the cantilever member where failure occurred.

Hysteretic Behavior and Damage Evolution

RC Member

The control RC specimen exhibited a stable hysteretic behavior up to approximately 4.0% drift, sustaining a peak shear stress of 2.1 MPa ($0.35\sqrt{f'_c}$). After being subjected to one cycle to a peak drift of 5.0% in the positive loading direction, the specimen exhibited a significant shear strength decay [Fig. 6(a)] due to severe concrete deterioration in the plastic hinge regions (Fig. 7). Minor "pinching" in the hysteresis loops can be observed for the cycles performed up to approximately 3.0% drift. For cycles at larger drift levels, this pinching increased as diagonal cracks opened widely. Damage during low drift levels (up to 1.0% drift) consisted primarily of hairline flexural and flexural-shear cracks with widths not exceeding 0.25 mm. In this and all other test specimens, first yielding of the longitudinal reinforcement occurred during or before the cycles at 1.0% drift. At 2.0% drift, however, damage became significant, as the width in a few diagonal and flexural cracks exceeded 0.75 mm. Strain gauge readings and cracking pattern indicated that flexural inelastic deformations spread over the assumed plastic hinge length (effective beam depth d). During the cycles to 3.0% drift and larger, damage in the plastic hinge regions was severe, characterized by wide cracks and concrete spalling, as shown in Fig. 7. At the end of the test, both transverse and longitudinal reinforcement were exposed in the plastic hinge region, and damage was considered to be beyond repair.

FRCC Members without Web Reinforcement

Five out of the eight test specimens did not contain transverse steel reinforcement in order to evaluate the contribution from various FRCC materials to shear strength in members subjected to inelastic displacement reversals. As mentioned earlier, two fiber types were used in these specimens: (1) ultrahigh molecular weight polyethylene (PE) fibers and (2) steel hooked fibers, both in either 1.5 or 2.0% volume fraction. Results from direct tension tests indicated that the composites reinforced with PE fibers in either 1.5 or 2.0% volume fraction and steel hooked fibers in a 2.0% volume fraction exhibited a strain-hardening behavior. On the other hand, the fiber cement composite with 1.5% volume fraction of steel hooked fibers exhibited a strain-softening behavior [Fig. 4(b)]. The first specimen tested in this series was Specimen PE2.0-0-0.6, in which relatively low shear stress levels (peak stress of 1.6 MPa or $0.21\sqrt{f'_c}$) were induced at flexural yielding. This specimen exhibited a behavior dominated by flexure with negligible shear-related damage. A stable hysteretic behavior was observed up to approximately 5.0% drift [Fig. 6(b)], the displacement at which buckling of the longitudinal reinforcement became evident. At this drift level, tensile strains as large as 4.0% were

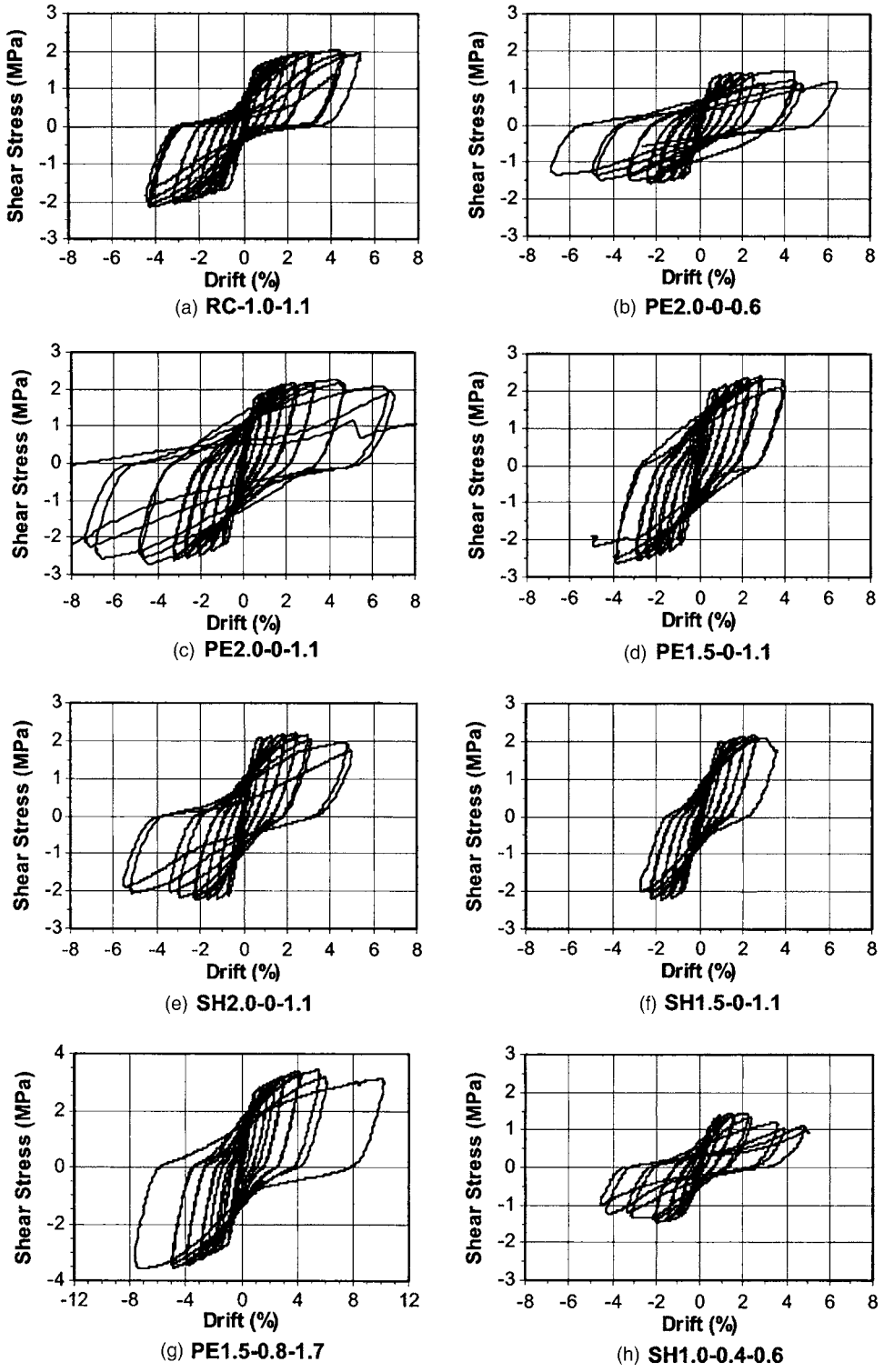

Fig. 6. Shear stress versus drift response (failure side)

measured in the longitudinal reinforcement at $d/2$ from the middle block face. Failure occurred during the cycle to 7.0% drift due to fracture of the longitudinal reinforcement at the beam-middle block interface.

Because the peak shear stress induced in Specimen PE2.0-0-0.6 would only represent a lower bound for the shear strength of flexural members with 2.0% volume fraction of PE fibers, an "identical" specimen, but with a nearly 50% increase in the area of longitudinal reinforcement, PE2.0-0-1.1, was tested in order to increase the shear stress demand at ultimate flexural capacity. Fig. 6(c) shows the shear stress versus drift response for this specimen. As shown in the figure, a very similar behavior compared to Specimen PE2.0-0-0.6 was observed. This specimen sustained two cycles at 7.0% drift, failing after reaching 10% drift in the negative loading direction due to fracture of the longitudinal reinforcement. The peak shear stress sustained by Specimen

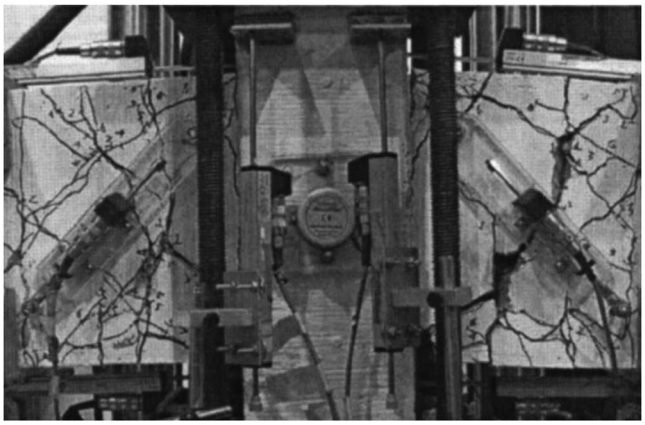

Fig. 7. Damage in plastic hinge regions of Specimen RC-1.0-1.1 at 4.0% drift

PE2.0-0-1.1 was 2.7 MPa, which corresponded to $0.41\sqrt{f'_c}$ [MPa]. Minor damage was observed in this specimen up to 2.5% drift. As the drift was increased, a wide flexural crack at the beam-middle block interface started opening, but damage in the plastic hinge region was still minor [Fig. 8(a)]. It is worth mentioning that no signs of buckling of the longitudinal reinforcement were observed up to 5.0% drift. At this drift level, however, a crack along the longitudinal bars formed, causing the FRCC material to become less effective for providing lateral support to the longitudinal reinforcement. Bar buckling ultimately occurred at 7.0% drift [Fig. 8(b)], followed by reinforcement fracture after a drift of 10% was reached.

Given that no shear failure occurred in Specimen PE2.0-0-1.1 at shear stress levels as large as 2.7 MPa, an "identical" specimen, except for the use of a lower volume fraction of PE fibers (1.5%), was also tested (PE1.5-0-1.1). Up to 3.0% drift, damage in this specimen was minor with no signs of buckling of the beam longitudinal reinforcement. During the first cycle to 4.0% drift, a flexural crack at the beam-middle block interface opened widely and propagated diagonally towards the extreme tension fibers of the beam. This major crack further propagated along the longitudinal tension (top) reinforcement during the second cycle to that drift level, making the FRCC cover ineffective for confining the longitudinal reinforcement. However, no strength deterioration had occurred up to this stage, as indicated by the hysteretic behavior shown in Fig. 6(d). Significant buckling of the top longitudinal reinforcement occurred during the first cycle to 5.0% drift, leading to the termination of the test.

The behavior of members with steel hooked fiber reinforced cement composites without web reinforcement was evaluated through the tests of two specimens, SH2.0-0-1.1 and SH1.5-0-1.1. Specimen SH2.0-0-1.1, with 2.0% volume fraction of steel hooked fibers, behaved well up to 5.0% drift [Fig. 6(e)]. Minor damage was observed up to the cycles to 2.0% drift. At 2.5% drift, a large flexural-shear crack in the left beam region near the middle block opened, and at 5.0% drift, extensive flexural damage, which included buckling of the beam longitudinal bars in the right beam element [Fig. 9(a)], was observed. During the cycles to this drift level, the hysteresis loops became pinched [Fig. 6(e)] due to sliding along large flexural cracks and extensive buckling of the reinforcement. The test was terminated after two full cycles to 5.0% drift.

The behavior of Specimen SH1.5-0-1.1, with 1.5% volume fraction of steel hooked fibers, was stable only up to 2.5% drift [Fig. 6(f)], with moderate flexural and shear cracking. During the first cycle to 3.0% drift, however, a diagonal tension failure occurred in the left beam member [Fig. 9(b)], leading to the termination of the test. It is worth mentioning that the FRCC material with 1.5% volume fraction of steel hooked fibers exhibited a strain-softening behavior under direct tension [Fig. 4(b)], as opposed to the strain-hardening behavior with multiple cracking observed in the composite with 2.0% volume fraction of steel hooked fibers. The two specimens with steel hooked fibers sustained the same peak shear stress demand of 2.2 MPa, but the test results suggest that the use of a strain-hardening composite is required to ensure adequate displacement capacity at that shear stress level in members without web reinforcement.

FRCC Members with Web Reinforcement

Two FRCC test specimens were reinforced with hoops in order to evaluate the interaction between the FRCC and steel shear resisting mechanisms. One specimen was constructed with a mortar FRCC containing PE fibers in a 1.5% volume fraction (Specimen PE1.5-0.8-1.7), while the other specimen contained regular concrete with 1.0% volume fraction of steel hooked fibers (SH1.0-0.4-0.6). Specimen SH1.0-0.4-0.6 was tested to evaluate whether the use of a low fiber volume fraction in combination with regular concrete would allow an increase in hoop spacing in plastic hinge

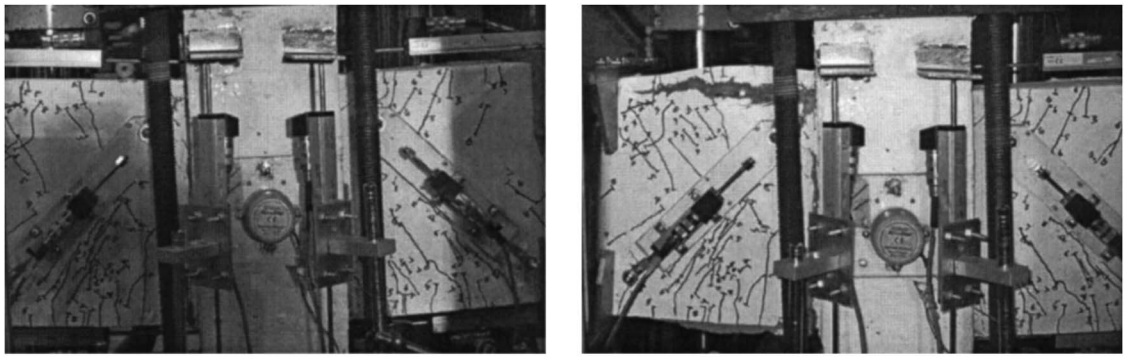

(a) **Cracking pattern at 4.0% drift**

(b) **Buckling of top longitudinal reinforcement at 7.0 drift**

Fig. 8. Damage in plastic hinge regions of Specimen PE2.0-0-1.1

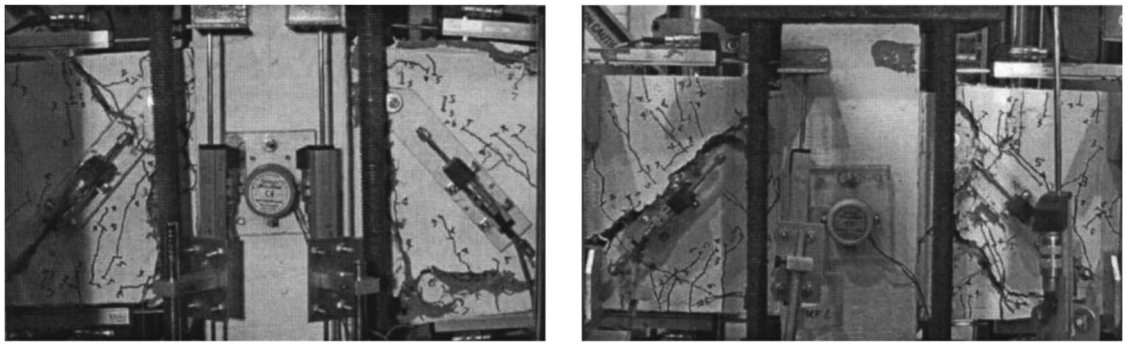

(a) **Specimen SH2.0-0-1.1 after two cycles at 4.0% drift**

(b) **Specimen SH1.5-0-1.1 after two cycles at 3.0% drift**

Fig. 9. Damage in FRCC specimens with steel hooked fibers

regions of flexural members. In both cases, transverse reinforcement was provided at a spacing, s, equal to half the beam effective depth, d. Detailed descriptions of these two specimens is given in Table 1.

The shear stress versus drift behavior of Specimen PE1.5-0.8-1.7 is shown in Fig. 6(g). This specimen sustained the largest shear stress demand among all the specimens (3.6 MPa) with a displacement capacity of approximately 6.0% drift. Ultimately, this specimen exhibited a diagonal tension failure at 10% drift. Specimen SH1.0-0.4-0.6, on the other hand, exhibited a modest performance, with a 30% strength decay at 4.5% drift. In this specimen, severe flexural damage, characterized by concrete crushing, bar buckling, and 8–15 mm wide flexural cracks, was observed during the cycles to 3.0 and 4.5% drift.

Buckling of Longitudinal Reinforcement

Figure 10 shows a plot indicating the plastic hinge rotation levels at which: (1) a longitudinal splitting crack along the beam reinforcement was first observed, and (2) buckling of longitudinal reinforcement was evident [comparable to that in Fig. 8(b)] in the specimens without hoops. As can be seen, cracks along the longitudinal reinforcement were first observed at plastic hinge rotations ranging from 1.8 to 4.3%. However, buckling was only evident at plastic hinge rotations of 4.0% or greater, which suggests that the FRCC materials provided adequate confinement to prevent buckling of longitudinal reinforcing bars in the test specimens at inelastic rotation levels expected during a major earthquake event.

No signs of compression-related damage or buckling were observed in Specimen PE1.5-0.8-1.7, with a strain-hardening FRCC and transverse reinforcement spaced at half the member effective depth. However, Specimen SH1.0-0.4-0.6, with regular concrete and 1.0% volume fraction of steel hooked fibers, exhibited substantial concrete crushing in the region adjacent to the middle loading block and slight bar buckling between the first and second hoop at 3.0% drift. These results indicate that spacing requirements for transverse reinforcement cannot be relaxed when regular concrete with 1.0% volume fraction of steel hooked fibers is used.

Evaluation of Member Shear Strength

Shear Resistance Contribution from FRCC Materials

One of the main purposes of using FRCC materials in plastic hinge regions of flexural members is to delay shear strength decay under large inelastic displacement reversals. In flexural members constructed with FRCC materials, randomly distributed fibers enhance shear resistance by providing post-cracking diagonal tension resistance, and by reducing diagonal crack width, which enhances aggregate interlock. The increase in shear resistance observed in fiber-reinforced concrete members has been accounted for by assuming a diagonal tension resistance equal to the FRCC post-cracking strength (Khuntia et al. 1999). This requires a conservative estimation of the post-cracking strength of the FRCC material, which for the case of strain-softening composites, could be substantially lower than the first cracking strength. In strain-hardening FRCC materials, however, the post-cracking strength is greater than the first cracking strength and thus, their tensile behavior could be conservatively assumed as perfectly plastic from first cracking up to damage localization. In this case, the use of a parameter known to correlate well with the first cracking strength of concrete, such as $\sqrt{f'_c}$, would provide a convenient way for evaluating the shear resistance of strain-hardening FRCC members. In addition, the use of $\sqrt{f'_c}$ allows easy comparison with shear strength equations used in design of RC members.

In order to estimate the shear stress at which a significant deterioration of shear resisting mechanisms occurred, a plot of the ratio between average shear strain, γ, and flexural rotation, θ, in the plastic hinge region (γ/θ) versus shear stress, v_c, in $\sqrt{f'_c}$, [MPa], is shown in Fig. 11. Fig. 11(a) concentrates on strain-hardening FRCC specimens without web reinforcement, while Fig. 11(b) shows the behavior of the specimens with transverse

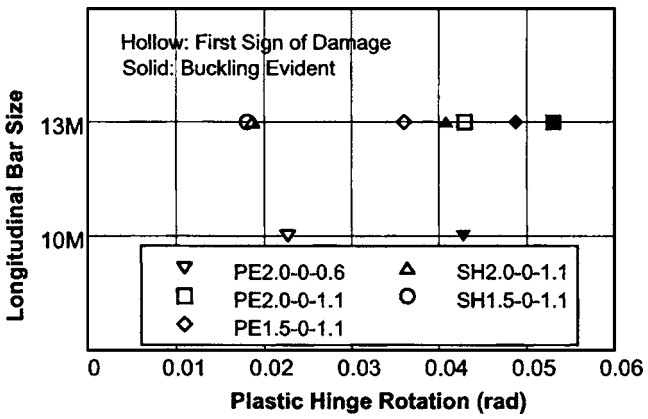

Fig. 10. Plastic hinge rotations at buckling of longitudinal reinforcement (specimens without hoops)

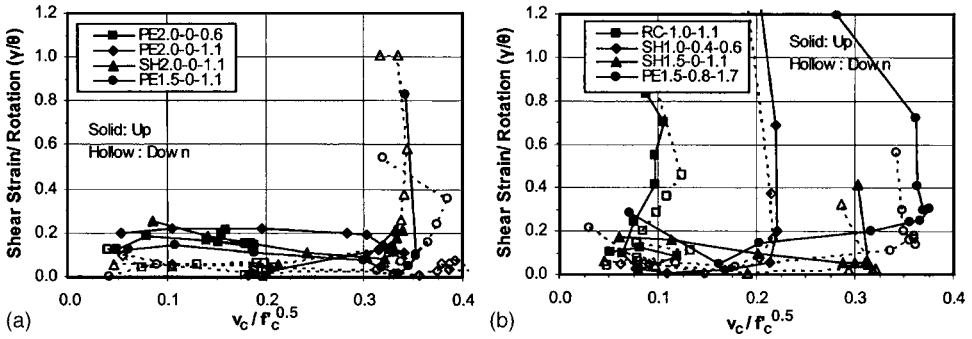

Fig. 11. Relative plastic hinge deformations versus shear stress: (a) specimens with strain-hardening FRCC and no hoops; (b) specimens with strain-softening FRCC and/or hoops

reinforcement and/or strain-softening FRCC. In this figure, the data corresponding to displacement half-cycles in the upward and downward directions have been indicated by solid and hollow markers, respectively. As shown in Fig. 11(a), two types of responses were observed for the strain-hardening FRCC specimens. For those members failing in flexure without noticeable shear damage, such as Specimen PE2.0-0-1.1, the γ/θ ratio remained at or below 0.25 for shear stress levels of up to $0.40\sqrt{f'_c}$ [MPa]. On the other hand, the specimens exhibiting a shear failure, or substantial shear damage at flexural failure, exhibited a sharp increase in the γ/θ ratio at shear stress levels ranging between 0.32 and $0.35\sqrt{f'_c}$ [MPa], indicating a rapid shear stiffness decay in the beam plastic hinge region.

With regard to the RC control specimen and Specimen SH1.0-0.4-0.6 [Fig. 11(b)], a similar trend was observed, but the sharp decay in shear stiffness began at shear stress levels of 0.12 and $0.21\sqrt{f'_c}$ [MPa], respectively. It should be mentioned that the shear stresses referred to in Fig. 11(b) correspond to those assigned to the concrete, v_c, which were determined by subtracting the shear stress carried by the hoops (estimated from strain gauge data) from the total applied shear and assuming a 60 degree angle for the diagonal compression struts, as will be explained later. It is interesting to note that even though Specimen SH1.5-0-1.1 was constructed with a strain-softening material, it did not show a significant shear stiffness deterioration up to shear stress levels slightly greater than $0.30\sqrt{f'_c}$ [Fig. 11(b)]. With regard to Specimen PE1.5-0.8-1.7, with a strain-hardening FRCC and hoops, a behavior consistent with that of strain-hardening FRCC members without transverse steel reinforcement was observed, with γ/θ ratios below 0.25 up to a shear stress level of $0.36\sqrt{f'_c}$.

From Fig. 11(a), it is seen that the ratio between shear distortion and plastic hinge rotation remained relatively constant up to a shear stress slightly greater than $0.30\sqrt{f'_c}$ in all strain-hardening FRCC specimens without web reinforcement, indicating that no significant stiffness degradation had occurred in the FRCC shear resisting mechanisms up to that stress level. The plot shown in Fig. 11(a), however, only gives an indication of the magnitude of the shear stresses at which a significant decay in shear stiffness occurred, but not of the magnitude of shear strains and plastic hinge rotations. Thus, the plastic hinge rotation versus shear distortion response for all the specimens constructed with strain-hardening FRCCs is shown in Figs. 12(a and b) for shear stress levels below and above $0.30\sqrt{f'_c}$, respectively. For shear stress levels below $0.30\sqrt{f'_c}$, the shear strains remained below 0.5% (minor damage) at plastic hinge rotations of up to 9.0% [outside the scale of Fig. 12(a)]. For shear stresses above $0.30\sqrt{f'_c}$ [Fig. 12(b)], on the other hand, a significant scatter in the data can be observed, with a shear strain of 0.5% at plastic hinge rotations ranging between 2.0 and 5.0%.

From the discussion above and based on the limited test data, a shear stress level of $0.30\sqrt{f'_c}$ [MPa] seems reasonable as a lower bound for the contribution from strain-hardening FRCC materials to member shear strength, regardless of the rotation demand. With

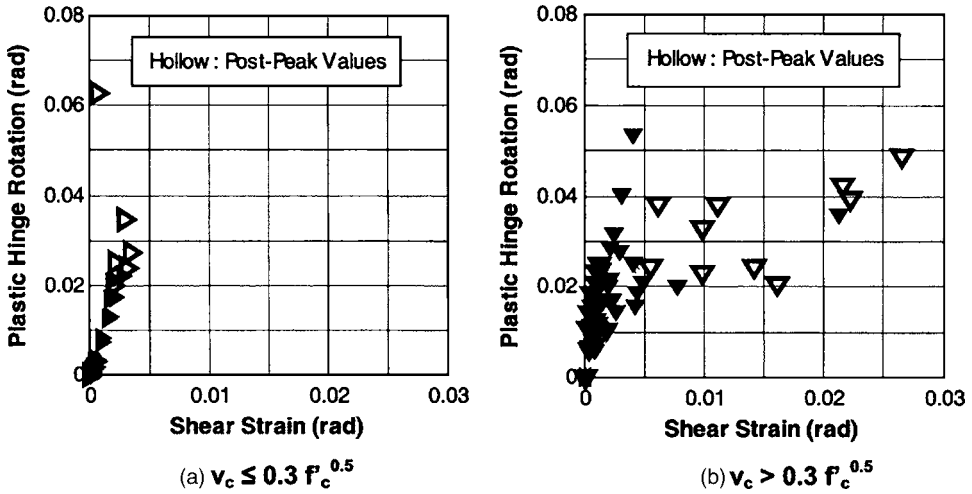

Fig. 12. Rotation versus average shear strain in plastic hinge region

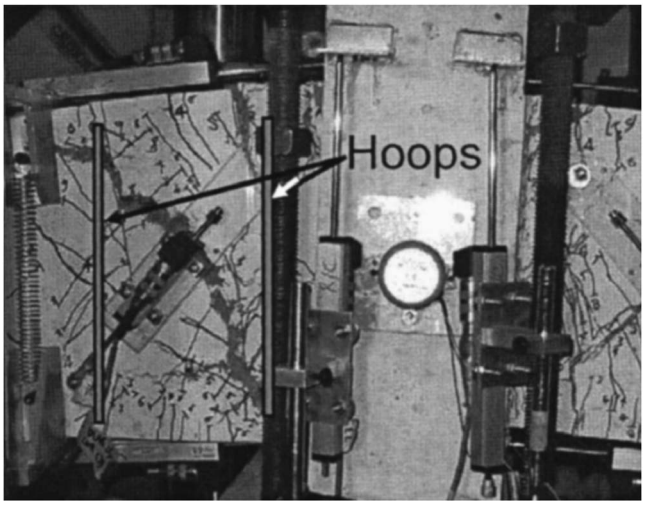

Fig. 13. Location of primary diagonal crack with respect to hoops (Specimen PE1.5-0.8-1.7)

regard to members with strain-softening FRCCs, the data presented in Fig. 11(b) indicate that the addition of fibers enhanced member shear resistance. However, the information available is very limited and thus, further studies are necessary to reliably quantify the shear strength contribution from strain-softening FRCC materials.

Shear Resistance of Transverse Steel Reinforcement

The contribution from transverse steel reinforcement to the shear strength of FRCC members was evaluated through strains measured in the hoops located in the plastic hinge regions of Specimen PE1.5-0.8-1.7, as well as through the angle of inclination and location of the primary diagonal crack that led to failure in the specimen. Specimen PE1.5-0.8-1.7 was used for this purpose because it was the only FRCC specimen containing hoops that exhibited a diagonal tension failure. The hoop strains in the regular concrete member, RC-1.0-1.1, were also measured for comparison purposes. Examining the cracking pattern in Specimen PE1.5-0.8-1.7 at failure, it was noted that only the second hoop, located at 170 mm from the left face of the middle block, was crossed by the primary diagonal crack (Fig. 13). This crack had an average angle of inclination of approximately 55 degrees with respect to the longitudinal member axis and terminated at the location of the first hoop (55 mm from the middle block face). A similar diagonal crack angle was observed in the RC specimen (right side), but extended up to the face of the middle block (Fig. 7). It should be mentioned that inclined cracks with angles steeper than 45 degrees have been observed in RC members subjected to reversed cyclic loading (Paulay and Priestley 1992).

Evaluating the strains in the second hoop of Specimen PE1.5-0.8-1.7, a nearly linear relationship between strain and member drift was observed. At 5.0% drift, a peak tensile strain of 0.2% was measured in that hoop, compared to 3.0% in the RC specimen at the same drift level. After opening of the primary diagonal crack in Specimen PE1.5-0.8-1.7, the specimen was still able to maintain most of its strength due to the shear resistance provided through dowel action from the #16M longitudinal bars (1.7% tension reinforcement ratio). This mechanism was enhanced by the presence of the first hoop, as evidenced by a substantial increase in tensile strains after the opening of the primary diagonal crack, even though it was not crossed by that crack.

Based on the limited test results, the use of a 60 degree crack angle, measured with respect to the member longitudinal axis and originating from the location of a hoop, seems reasonable for estimating the contribution of transverse steel reinforcement to shear strength in plastic hinge regions of FRCC flexural members. Thus, the nominal shear strength of these members, V_n, can be estimated as

$$V_n = 0.30\sqrt{f'_c}b_w d + A_v f_{yv} n_v \quad (1)$$

where f'_c is the FRCC compressive strength [MPa], b_w is the member web width, d is the member effective depth, A_v and f_{yv} are the transverse reinforcement area (one layer) and yield strength, respectively, and n_v is the number of layers of hoops and crossties (whole number) crossed by a 60 degree angle diagonal crack assumed to originate at the location of a hoop layer. Using Eq. (1), a peak total shear stress of 2.9 MPa was predicted for Specimen PE1.5-0.8-1.7, which represents 83% of the peak shear stress of 3.5 MPa measured at 5.0% drift.

Summary and Conclusions

Results from reversed cyclic displacement tests of flexural members constructed with fiber-reinforced cement composites (FRCCs) were presented, with an emphasis on the evaluation of member displacement capacity and shear strength. From the results presented, the following conclusions can be drawn:

1. All strain-hardening FRCC test specimens, with or without transverse steel reinforcement, exhibited a stable behavior with drift capacities equal to or greater than 4.0%. Peak shear stress demands in the test specimens without web reinforcement ranged from $0.21\sqrt{f'_c}$ to $0.40\sqrt{f'_c}$ [MPa], and it was equal to $0.51\sqrt{f'_c}$ for the strain-hardening FRCC member with web reinforcement. Compared to a control RC member designed according to Chapter 21 of the 2002 ACI Building Code, the strain-hardening FRCC specimens exhibited superior damage tolerance with multiple flexural and diagonal cracking.
2. A shear stress level of $0.30\sqrt{f'_c}$ [MPa] represented a lower bound for the shear resistance provided by strain-hardening FRCCs in the test specimens, regardless of the level of inelastic rotation demand. All strain-hardening FRCC specimens that exhibited a shear failure and/or a significant decay in shear stiffness were subjected to shear stresses greater than $0.30\sqrt{f'_c}$.
3. Buckling of longitudinal reinforcement in the strain-hardening FRCC specimens without web reinforcement was only evident after a 4.0% plastic hinge rotation was reached, while no buckling was observed in a specimen with web reinforcement spaced at half the member effective depth. This suggests that strain-hardening FRCC materials were effective in providing lateral support to the longitudinal reinforcement in the test specimens.
4. Based on the limited test results, the use of a 60 degree crack angle, measured with respect to the member longitudinal axis and originating from the location of a hoop, seems reasonable for estimating the contribution of transverse steel reinforcement to shear strength in plastic hinge regions of FRCC flexural members.

Acknowledgments

The research described herein was partially sponsored by the National Science Foundation under Grant No. CMS 0324519. The opinions expressed in this paper are those of the writers and do not necessarily reflect the views of the sponsors. The writers would also like to acknowledge the support and suggestions of Professor Antoine E. Naaman and Professor James K. Wight. Dramix fibers used in this investigation were generously donated by Bekaert Corp.

References

ACI Committee 318. (2002). "Building code requirements for structural concrete." *Rep. No. ACI 318-02*, American Concrete Institute, Farmington Hills, Mich.

Aschheim, M., and Moehle, J. P. (1992). "Shear strength and deformability of RC bridge columns subjected to inelastic cyclic displacements." *Rep. No. UCB/EERC-92/04*, Earthquake Engineering Research Center, Univ. of Calif. at Berkeley, Berkeley, Calif.

Adebar, P., Mindess, S., St.-Pierre, D., and Olund, B. (1997). "Shear tests of fiber concrete beams without stirrups." *ACI Struct. J.*, 94(1), 68–76.

Batson, G., Jenkins, E., and Spatney, R. (1972). "Steel fibers as shear reinforcement in beams." *ACI J.*, 69(10), 640–644.

Bayasi, Z., and Gebman, M. (2002). "Reduction of lateral reinforcement in seismic beam-column connection via application of steel fibers." *ACI Struct. J.*, 99(6), 772–780.

Blume, J. A., Newmark, N. M., and Corning, L. H. (1961). *Design of multistory reinforced concrete buildings for earthquake motions*, Portland Cement Association, Skokie, Ill.

Craig, R., Mahadev, S., Patel, C., Viteri, M., and Kertesz, C. (1984). "Behavior of joints using reinforced fibrous concrete." *ACI SP-81*, American Concrete Institute, Detroit, 125–167.

Filiatrault, A., Pineau, S., and Houde, J. (1995). "Seismic behavior of steel-fiber reinforced concrete interior beam-column joints." *ACI Struct. J.*, 92(5), 543–552.

Fischer, G., and Li, V. C. (2002). "Effect of matrix ductility on deformation behavior of steel-reinforced ECC flexural members under reversed cyclic loading conditions." *ACI Struct. J.*, 99(6), 781–790.

Gefken, P. R., and Ramey, M. R. (1989). "Increased joint hoop spacing in type 2 seismic joints using fiber reinforced concrete." *ACI Struct. J.*, 86(2), 168–172.

Henager, C. H. (1977). "Steel fibrous, ductile concrete joint for seismic-resistant structures." *Reinforced concrete structures in seismic zones*, SP-53, American Concrete Institute, Detroit, 371–379.

Khuntia, M., Stojadinovic, B., and Goel, S. C. (1999). "Shear strength of normal and high-strength fiber reinforced concrete beams without stirrups." *ACI Struct. J.*, 96(2), 282–289.

Kwak, Y. -K., Eberhard, M. O., Kim, W.-S., and Kim, J. (2002). "Shear strength of steel fiber-reinforced concrete beams without stirrups." *ACI Struct. J.*, 99(4), 530–538.

Lehman, D. E., Lynn, A. C., Aschheim, M. A., and Moehle, J. P. (1996). "Evaluation methods for reinforced concrete columns and connections." *Proc. 11th World Conf. on Earthquake Engineering*, Paper No. 673, Elsevier Science Ltd., Acapulco, Mexico.

Li, V. C. (1993). "From micromechanics to structural engineering—The design of cementitious composites for engineering applications." *J. Structural Mechanics and Earthquake Eng., JSCE, Japan*, 10(2), 37–48.

Li, V. C., Ward, R., and Hmaza, A. M. (1992). "Steel and synthetic fibers as shear reinforcement." *ACI Mater. J.*, 89(5), 499–508.

Mansur, M. A., Ong, K. C. G., and Paramasivam, P. (1986). "Shear strength of fibrous concrete beams without stirrups." *J. Struct. Eng.*, 112(9), 2066–2079.

Martín-Pérez, B., and Pantazopoulou, S. J. (1998). "Mechanics of concrete participation in cyclic shear resistance of RC." *J. Struct. Eng.*, 124(6), 633–641.

Mishra, D., and Li, V. C. (1995). "Performance of a ductile plastic hinge designed with an engineered cementitious composite." *UMCEE Rep. No. 95-06*, Dept. of Civil and Environmental Engineering, Univ. of Mich., Ann Arbor, Mich.

Naaman, A. E., and Reinhardt, H. W. (1996). "Characterization of high performance fiber reinforced cement composites—HPFRCC." *High Performance Fiber Reinforced Cement Composites 2, Proc., 2nd Int. RILEM Workshop*, A. E. Naaman and H. W. Reinhardt, eds., E & FN Spon, Ann Arbor, Mich., 1995, 1–24.

Narayanan, R., and Darwish, I. Y. S. (1987). "Use of steel fibers as shear reinforcement." *ACI Struct. J.*, 84(3), 216–227.

Paulay, T., and Priestley, M. J. N. (1992). *Seismic design of reinforced concrete and masonry buildings*, Wiley, New York.

Priestley, M. J. N., Verma, R., and Xiao, Y. (1994). "Seismic shear strength of reinforced concrete columns." *J. Struct. Eng.*, 120(8), 2310–2329.

Pujol, S. (2002). "Drift capacity of reinforced concrete columns subjected to displacement reversals." Ph.D. thesis, Purdue Univ.

Scribner, C. F., and Wight, J. K. (1980). "Strength decay in R.C. beams under load reversals." *J. Struct. Div.*, 106(4), 861–876.

Shantz, B. (1993). "The effect of shear stress in full-scale steel fiber reinforced concrete beams." MS thesis, Clarkson Univ., Potsdam, New York.

Wight, J. K., and Sozen, M. A. (1975). "Strength decay of RC columns under shear reversals." *J. Struct. Div.*, 101(5), 1053–1065.